Periodic oscillation of a colloidal disk near a wall in an optical trap

Zhengdong Cheng,[1,*] Thomas G. Mason,[1,†] and P. M. Chaikin[2]
[1]*Corporate Strategic Research, ExxonMobil Research and Engineering Company, Route 22 East, Annandale, New Jersey 08801, USA*
[2]*Department of Physics, Princeton University, Jadwin Hall, Princeton, New Jersey 08544, USA*
(Received 9 July 2003; published 25 November 2003)

Colloidal disks can be stably trapped using optical tweezers. However, when the tweezers press the disk against an opposing wall, we observe an instability leading to periodic motion which we model using coupled nonlinear equations. The resulting ''switchback'' oscillation involves combined orientational and translational motion of the disk. This observation reveals a new degree of freedom in colloidal architectures, that is, the ability to drive translational motion from a static light field energy source.

DOI: 10.1103/PhysRevE.68.051404 PACS number(s): 82.70.Dd, 87.80.Cc, 05.45.Xt

The dynamics of a dielectric object in a strongly focused Gaussian laser beam has been intensively studied. One of the important discoveries is the existence of a stable focus solution to the differential equations governing the motion of the object. This is the well-known optical trapping technique, or laser tweezers [1–4]. In previous work we have demonstrated that disks can be stably trapped ''edge-on'' to the direction of light propagation (flat surface perpendicular to the objective lens). Moreover, we found that the disk could be rotationally pinned or controllably rotated in linearly or circularly polarized light, respectively. We also observed a ''switchback'' oscillation when the trapped disk was forced against a wall [5].

In this paper we continue the study of an optically trapped disk in linearly polarized light when the trapping point is shifted toward the opposing cover slip in the microscope. This effectively pushes the edge-on disk against the wall. As we increase the pushing force an instability occurs which first tilts the disk face from perpendicular to the wall and at larger tilts, leads to periodic translation-tilt (orientational) motion. We present a simple dynamical model of the instability where the main elements are translational force from photon pressure on the tilted disk and a coupling torque which results from dragging the disk along the cover slip. The model can semiquantitatively explain the instability and its dependence on proximity to the wall and the laser power.

The ability to induce and control periodic translational motion, as well as rotation, with static light fields (i.e., without moving the laser tweezers) should enable the building of micron scale machines driven by a photon power source.

The microdisks were made by crystallizing α-eicosene wax $[CH_3—(CH_2)_{17}—CH{=}CH_2]$ aqueous emulsion particles. The right circular cylindrical disks arise when the cooled wax enters a lamellar liquid crystalline rotator phase that occurs at 29.8 °C [6]. The lamellar planes lie parallel to the flat faces, and the in-plane orientational disorder of wax molecules facilitates an in-plane isotropic surface energy that permits a circular perimeter. The microdisks have radii ranging from 0.2 to 10 μm and aspect ratios ranging from 2 to 10 with $\rho = 5$ typically. Attractive depletion forces [7], induced by raising the sodium dodecyl sulfate (SDS) concentration above the critical micelle concentration, are repeatedly used to preferentially segregate the disks from other spherical objects. The shape selectivity is possible due to the much larger excluded volume between two disks oriented face-to-face as compared to the much smaller volume between a disk and a sphere. Under differential interference contrast (DIC) microscopy, the disks appear to be birefringent.

Our laser tweezers consist of an inverted microscope with an expanded laser beam that enters the microscope through the epifluorescence port and is bounced upward into the 100×1.4 NA oil-immersion objective by a dichroic mirror. Green illumination passes through the condenser lens in the direction opposite to the laser beam. We use either a 15-mW He-Ne laser at a wavelength of $\lambda = 633$ nm, or, for additional power, a 10-W solid state Nd:YAG (yttrium aluminum garnet) laser at $\lambda = 1064$ nm. Both lasers are linearly polarized. Strikingly, all disks are trapped stably in three dimensions, regardless of radius or aspect ratio even for those approaching the microscope's resolution limit of 0.2 μm. They align edge-on with their faces parallel to the beam axis, thereby maximizing the disk's volume in the region of highest electric field, Fig. 1. The linear polarized laser beam creates a harmonic restoring torque that causes the disk's faces to lie along the polarization direction [8–10]. By changing the polarization direction, the in-plane orientation of its symmetry axis can be controlled. Disks can be manipulated in the z direction without disturbing their orientation by adjusting the focus. Thermal fluctuations cause higher amplitude translational excursions of the center of the disk along its edge as compared to its symmetry axis. For small laser powers at which the disk is barely trapped translationally, the disk also exhibits significant rocking orientational fluctuations, causing its symmetry axis to deviate from the focal plane so that it is not always oriented completely edge-on. For details and the technique using scattering light to measure the rotational motion of the disk, please refer to our previous publication [5].

We focus here on the interesting dynamic Hopf bifurcation and resulting switchback motion. A confining wall can alter the stability of a disk in the linearly polarized tweezers. When a disk is moved in the z direction so that it becomes perturbed by the glass wall, the disk tilts and begins to trans-

*Present address: ESL 202, DEAS, Harvard University, 40 Oxford St., Cambridge, MA 02138.
Email address: zcheng@deas.harvard.edu
†Present address: Department of Chemistry and Biochemistry and Department of Physics, University of California–Los Angeles, 3040 Young Hall, 607 Charles E. Young Dr. East, Box 951569, Los Angeles, CA 90095-1569, USA.

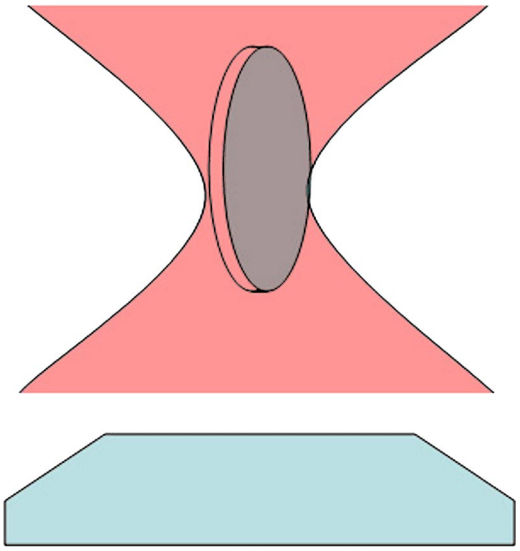

FIG. 1. (Color online) Schematic diagram of a dielectric disk trapped "edge-on" in the focussed light field of an optical tweezer.

late in the direction perpendicular to the polarization direction, Fig. 2. We attribute this escaping motion to the driving force originating from the scattering of the laser from the tilted surface of the disk. As the disk moves there is a drag force on the edge closest to the wall. This introduces an additional torque increasing the tilt. As the disk moves from the beam center there is a lateral restoring force from the electric field gradient. At the far end of the traverse, the velocity decreases, the viscous torque arising from wall-disk interaction decreases and the alignment torque of the tweezers causes the disk to again align edge-on. In this configuration there is no longer a lateral scattering force and the disk is drawn back toward the beam center by the field gradients (the usual trapping force). The reverse motion causes a reverse tilt via the wall-disk interaction torque and the disk accelerates in the opposite direction through the beam center. This process repeats creating a coupled translational-orientational "switchback" oscillation.

The successive micrographs (1–6) in Fig. 2(a) show the oscillation of the disk (radius 1.5 μm) in a linearly polarized laser tweezer at a He-Ne laser power of $P=8$ mW when the

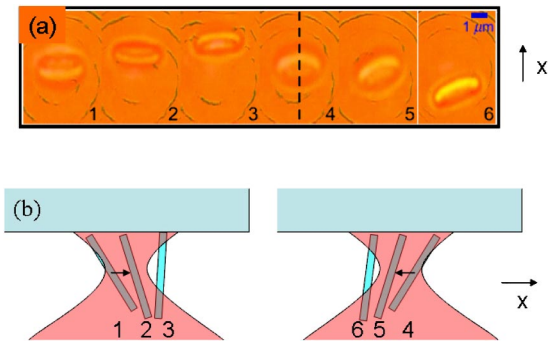

FIG. 2. (Color online) "Switchback" oscillation of a short-cylindrical disk in the optical tweezers, near an opposing wall. (a) Time sequence images (1–6) with one-sixth of a second apart. (b) Schematics of the motion 1-2-3-4-5-6 (1).

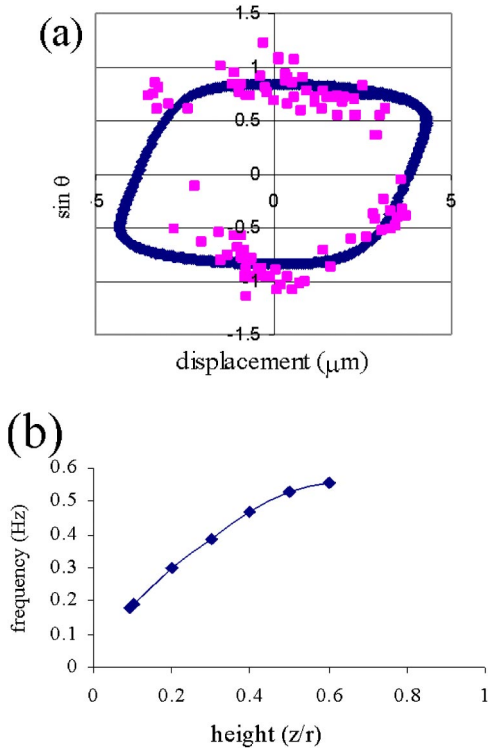

FIG. 3. (Color online) (a) Lissajou pattern for $x(t)$ and $\sin\theta(t)$ from numerical integration and experimental measurement ($z=0.2r$). (b) Disk-wall separation dependence of the "switchback" frequency. (There are no oscillations for $z>z_c\sim0.64r$.) Note that the frequency jumps discontinuously at z_c characteristic of a supercritical Hopf bifurcation.

focal plane is ~1 μm away from the slide surface; frames are one-sixth of a second apart. Figure 2(b) shows a cartoon of the motion viewed perpendicular to the motion and the light beam. This type of oscillation, where the orientation of the disk plays a key role, does not occur for the trapped microspheres near glass surfaces for the reasons of symmetry. The frequency of the microdisk's switchback oscillation is proportional to the laser power, inversely proportional to the viscosity, and depends on the position of the focal plane relative to the glass surface. The frequency increases linearly with laser power, $f_s\sim P$, and it becomes smaller near the glass slide due to increased viscous forces and a reduction in the volume of the disk in the region of highest electric field intensity. The amplitude of the translational excursion and the tilt angle diminish as the distance between the slide and focal plane increases.

To extract quantitative information, the projections of the circular surfaces of the disk on the focal plan were measured by processing these micrographs. IDL (Research Systems) was used to define the projection and calculate the coordinates of the disk's center (x,y) and projection area was used to measure the orientation angle θ. Figure 3(a) shows the scatter plot of $\sin\theta$ *vs* x. The solid line is the calculation according to the model presented below. The model gives a reasonable interpretation of the experimental observation.

We propose the following equations for the position x and tilt angle θ of the disk near the glass slide (note that θ here is

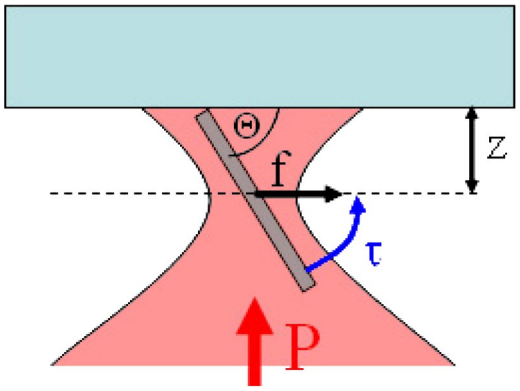

FIG. 4. (Color online) Geometry used for modelling the switchback motion. As the focus is shifted toward the opposing wall the disk tilts, photons scatter from the disk surface and initiate a lateral force and motion.

different from the rotation angle θ that we defined in our previous publication):

$$a_1 p \sin\theta\cos\theta - a_2 p x - a_3 \frac{dx}{dt} = 0,$$

$$a_4 r p \sin\theta(r\cos\theta - z) - a_5 p \sin\theta\cos\theta + a_6 \cos\theta(r\cos\theta - z)\frac{dx}{dt} - a_7 \frac{d\theta}{dt} = 0, \qquad (1)$$

where p is the laser power. The geometry for these calculations is shown schematically in Fig. 4. The first equation describes the force equilibrium in the horizontal direction x. The term a_1 is from the radiation force originating from the scattering of the light when the disk tilts. The coefficient a_1 is proportional to the area of the disk and its reflectivity. θ is the angle between the symmetric axis of the disk and the vertical z direction. The term a_2 is the gradient force that traps the disk horizontally. We use a harmonic approximation with $a_2 p$ proportional to the stiffness of the trapping force. The term a_3 is the viscous damping term proportional to the disk radius and the fluid viscosity.

The second equation describes the torque equilibrium in a horizontal direction that is perpendicular to x. The term a_4 comes from the force with which the tweezers push the disk into the wall. If the disk is tilted, there is a lever arm for this force and hence a torque. This term is necessarily zero when the disk is not touching the wall. The coefficient $a_4 p$ is proportional to the trapping force constant in the z direction. The term a_5 is from the torque of the tweezers which causes the symmetric axis of the disk to align horizontally, disk edge-on to the objective, Fig. 1. The coefficient a_5 depends on the shape anisotropy of the disk. The term a_7 is from the viscous damping of the rotation in the tilt direction. The coefficient a_7 is proportional to the disk radius cubed. The term a_6 is the most interesting. Without this term the orientation and translation are decoupled and there is no oscillation. The coupling results from the different viscous stress on the region of a particle close to a wall as opposed to far from the wall as the particle translates parallel to the wall. The edge-on disk, moving near a wall, will have more drag along the almost touching edge. The result is a torque which increases the tilt. It is similar to the torque which would result from friction of a touching edge on the wall. Although the torque resulting from this edge-wall interaction is a complex function of the distance from the disk center to the wall, we take an approximate simplified form, proportional to the distance between the wall and disk center. a_6 depends on the viscous drag coefficient of the disk.

The force generated by the laser beam p is proportional to the power. We adopt units such that p is measured in pN (a 1-mW laser generates a force ≈ 1 pN), and define $r \sim 1$ μm as the disk radius $D_x \sim 1$ μm as the half width of the laser beam at focus, $D_z \sim 1$ μm as the characteristic length for the intensity gradient along z. The coefficients of each term are then $a_1 \sim (\pi r^2/\pi D_x^2)$, $a_2 \sim D_x^{-1}$, $a_3 \sim 6\pi\eta r$, $a_4 \sim D_z^{-1}$, $a_5 \sim r$, $a_6 \sim 6\pi\eta r$, and $a_7 \sim 8\pi\eta r^3$.

We rewrite the equations as

$$\begin{pmatrix} \frac{dx}{dt} \\ \frac{d\theta}{dt} \end{pmatrix} = \begin{pmatrix} \frac{a_1 p \sin\theta\cos\theta - a_2 p x}{a_3} \\ \frac{a_4 r p \sin\theta(r\cos\theta - z) - a_5 p \sin\theta\cos\theta + a_6(r\cos\theta - z)\cos\theta \, \frac{a_1 p \sin\theta\cos\theta - a_2 p x}{a_3}}{a_7} \end{pmatrix}. \qquad (2)$$

For any periodic solution of this equation, the frequency will be proportional to the laser power, since p appears in all but the viscous damping terms. This is consistent with our experimental observations. We linearize this set of equations around its equilibrium point $(x,\theta) = (0,0)$.

$$\begin{pmatrix} \frac{dx}{dt} \\ \frac{d\theta}{dt} \end{pmatrix} = A \begin{pmatrix} x \\ \theta \end{pmatrix} = \begin{pmatrix} \frac{-a_2 p}{a_3} & \frac{p a_1}{a_3} \\ \frac{-a_2 a_6 (r - Z) p / a_3}{a_7} & \frac{a_4 r p (r - Z) - a_5 p + 2 p a_1 a_6 (r - Z)/a_3}{a_7} \end{pmatrix} \begin{pmatrix} x \\ \theta \end{pmatrix}. \qquad (3)$$

The eigenvalues of the matrix A are

$$\lambda_1 = \alpha + i\beta,$$

$$\lambda_2 = \alpha - i\beta, \tag{4}$$

where

$$\alpha = pa/2,$$

$$\beta = p\sqrt{|\Delta|}/2, \tag{5}$$

with

$$a = a_1 a_6 (r-z) + a_4 a_3 (r-z) - a_5 a_3 - a_2 a_6 (r-z),$$

$$\Delta = \left(\frac{a_2}{a_3} + \frac{[a_5 - a_4 r(r-z)]}{a_7} - \frac{a_1 a_6}{a_7 a_3} \right)^2 - 4\,\frac{a_2}{a_3}\left(\frac{[a_5 - a_4 r(r-z)]}{a_7} - \frac{a_1 a_6 (r-z)}{a_7 a_3} \right) - 4\,\frac{2a_1 a_6 (r-z)}{a_7 a_3}\,\frac{a_1}{a_3}. \tag{6}$$

The solution to Eq. (3) is

$$\begin{pmatrix} x \\ \theta \end{pmatrix} = e^{\alpha t} \begin{pmatrix} R_1 \cos(\beta t - \delta_1) \\ R_2 \cos(\beta t - \delta_2) \end{pmatrix}, \tag{7}$$

where R_1 and R_2 are not negative.

According to Eq. (7), the portrait of the solutions to Eq. (3) is determined by the sign of α. When $\alpha < 0$, the factor $e^{\alpha t}$ dictates that oscillating orbits decay with time. When $\alpha > 0$, static orbits are unstable and spiral away from the origin as for early times. Eventually the nonlinear terms become important and we may have stable oscillating solutions [11].

Since we are after the characteristic behaviors and instabilities rather than a detailed fit of our experimental observations we have chosen the following "reasonable" values for the coefficients in Eq. (1) in our numerical studies: $a_1 = 2$, $a_2 = 0.2\ \mu\text{m}^{-1}$, $a_3 = 1$ pN/(μm/s), $a_4 = 1\ \mu\text{m}^{-1}$ $a_5 = 1\ \mu$m, $a_6 = 1$ pNs, $a_7 = 1$ pN$-$s/(μm)^3, $d = 1\ \mu$m, and $p = 10$ pN. With this choice of coefficients, the only control parameter is the distance z of the center of the disk from the "wall," the upper cover slip. From Eqs. (5) and (6) we see that the instability occurs when $z < 0.643r = 0.643\ \mu$m. In Fig. 5(a) we take $z = 0.57r$ and plot the displacement and tilt angle which result from numerical integration of the equations of motion (1) with a small initial displacement and tilt. The oscillations grow and quickly saturate to a periodic orbit. Numerical and analytic solutions for $z > 0.643r$ at arbitrary initial conditions quickly decay to $x = 0$, $\theta = 0$. In Fig. 5(b) we show the experimentally measured disk displacement for a disk-wall separation of $\sim 1\ \mu$m. The image in Fig. 5(b) is obtained by plotting the microscope image of the disk along the dashed line in Fig. 2(a), frame 4, along the ordinate axis and time along the abscissa. Note that the displacement in both the experiment and the numerical integration are nonlinear, i.e., more triangle than the sine wave.

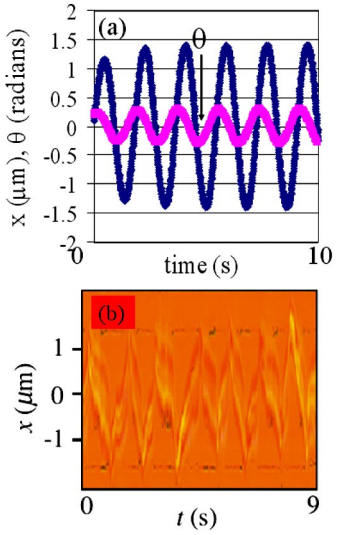

FIG. 5. (Color online) (a) Numerical integration of the equations of motion show coupled oscillations of displacement x (dark blue line) and tilt θ (light purple line) for parameters just inside instability regime. (b) Observed disk displacement as a function of time also shows anharmonic behavior, close to the critical disk-wall separation. [Time lapse image of the central section as indicated by the dashed line in Fig. 2(a).]

To see whether the model sufficiently captures the nature of the oscillation we have plotted in Fig. 3(a), a Lissajou pattern, $\sin\theta$ as a function of displacement, for the disk. The data is for a disk pressed closer to the wall than for Fig. 5 and the numerical integration is calculated for $z = 0.2r$. The data were obtained from images as in Fig. 2(a), analyzed for position from the centroid and tilt angle from the elliptical shape of the projection. The data and model are in quite good agreement. Note, however, that better agreement could be obtained by adjusting the many coefficients in Eq. (1), a task which is uncalled for given the crude nature of the model.

Since our experiments did not concentrate on detailed measurements of the disk-wall separation z we do not have quantitative data on the oscillation frequency as a function of z. We did note that the frequency decreased as the disk was pushed closer to the opposing cover slip. This tendency is also reflected in the numerical integration from which we obtain the plot in Fig. 3(b). We note that, as in other supercritical Poincare-Andronov-Hopf bifurcatons, the oscillation amplitude is continuous through the bifurcation point ($z/r = 0.643$), while the frequency discontinuously jumps to a finite value.

In summary, we have demonstrated experimentally and theoretically the onset of oscillatory dynamics for a dielectric object in optical tweezers. We expect that, with the developments in optics of laser tweezers (for example, Refs. [12–14]) as well as the shape control of colloids (see also, Ref. [15]), a variety of complex dynamic phenomena will be discovered in the near future. The fact that these can be characterized by simple models should enable construction of micron scale devices and machines, powered by static light sources.

We thank Matthew Sullivan for help in using of the infrared laser tweezers and Xunya Jiang for helpful discussions.

[1] A. Ashkin, J.M. Dziedzic, J.E. Bjorkholm, and S. Chu, Opt. Lett. **11**, 288 (1986).
[2] T.T. Perkins, D.E. Smith, R.G. Larson, and S. Chu, Science **268**, 83 (1995).
[3] *Laser Tweezers in Cell Biology*, edited by M. P. Sheetz, Methods in Cell Biology Vol. 55 (Academic, Orlando, 1998).
[4] R.C. Gauthier, J. Opt. Soc. Am. B **14**, 3323 (1997).
[5] Z. Cheng, P.M. Chaikin, and T.G. Mason, Phys. Rev. Lett. **89**, 108303 (2002).
[6] H. Gang *et al.*, J. Phys. Chem. B **102**, 2754 (1998).
[7] S. Asakura and F. Oosawa, J. Chem. Phys. **22**, 1255 (1954).
[8] P.L. Marston and J.H. Crichton, Phys. Rev. A **30**, 2508 (1984).
[9] M.E.J. Friese, T.A. Nieminen, N.R. Heckenberg, and H. Rubinsztein-Dunlop, Nature (London) **394**, 348 (1998).
[10] E. Higurashi, R. Sawada, and T. Ito, Phys. Rev. E **59**, 3676 (1999).
[11] M. Braun, *Differential Equations and Their Applications*, 4th ed. (Springer-Verlag, Berlin, 1992), p. 433.
[12] J.E. Curtis, B.A. Koss, and D.G. Grier, Opt. Commun. **207**, 169 (2002).
[13] V. Garces-Chavez *et al.*, Nature (London) **419**, 145 (2002).
[14] D. Grier *et al.*, Nature (London) **424**, 810 (2003).
[15] K.P. Velikov *et al.*, Appl. Phys. Lett. **81**, 838 (2002).